Aliphatic Carbonyl Compounds (C_8-C_{26}) in Wintertime Atmospheric Aerosol in London, UK

Ruihe Lyu[1,2], Mohammed Salim Alam[1], Christopher Stark[1]

Ruixin Xu[1], Zongbo Shi[1], Yinchang Feng[2] and Roy M. Harrison[†*1]

[1] Division of Environmental Health and Risk Management

School of Geography, Earth and Environmental Sciences, University of Birmingham Edgbaston, Birmingham B15 2TT, UK

[2] State Environmental Protection Key Laboratory of Urban Ambient Air Particulate Matter Pollution Prevention and Control, College of Environmental Science and Engineering

Nankai University, Tianjin 300350, China

† Also at: Department of Environmental Sciences / Centre of Excellence in Environmental Studies, King Abdulaziz University, PO Box 80203, Jeddah, 21589, Saudi Arabia.

Corresponding authors:
E-mail: r.m.harrison@bham.ac.uk (Roy M. Harrison)

ABSTRACT

Three groups of aliphatic carbonyl compounds, the n-alkanals (C_8-C_{20}), n-alkan-2-ones (C_8-C_{26}) and n-alkan-3-ones (C_8-C_{19}) were measured in air samples collected in London from January-April 2017. Four sites were sampled including two roof-top background sites, one ground-level urban background site and a street canyon location on Marylebone Road in central London. The n-alkanals showed the highest concentrations followed by the n-alkan-2-ones and the n-alkan-3-ones, the latter having appreciably lower concentrations. It seems likely that all compound groups have both primary and secondary sources and these are considered in the light of published laboratory work on the oxidation products of high molecular weight n-alkanes. All compound groups show relatively low correlation with black carbon and NOx in the background air of London, but in street canyon air heavily impacted by vehicle emissions, stronger correlations emerge especially for the n-alkanals. It appears that vehicle exhaust is likely to be a major contributor for concentrations of the n-alkanals whereas it is a much smaller contributor to the n-alkan-2-ones and n-alkan-3-ones. Other primary sources such as cooking or wood burning may be contributors for the ketones but were not directly evaluated. It seems likely that there is also a significant contribution from photo-oxidation of n-alkanes and this would be consistent with the much higher abundance of the n-alkan-2-ones relative to the n-alkan-3-ones if the formation mechanism were to be through oxidation of condensed phase alkanes. Vapour-particle partitioning fitted the Pankow model well for the n-alkan-2-ones but less well for the other compound groups, although somewhat stronger relationships were seen at the Marylebone Road site than at the background sites. The former observation gives support to the n-alkane-2-ones being a predominantly secondary product, whereas primary sources of the other groups are more prominent.

Keywords: Carbonyl compounds; n-alkanals; n-alkan-2-ones; n-alkan-3-ones; organic aerosol;

partitioning;

1. INTRODUCTION

Carbonyl compounds are classified as polar organic compounds, constituting a portion of the oxygenated organic compounds in atmospheric particulate matter (PM). Aliphatic carbonyl compounds are directly emitted into the atmosphere from primary biogenic and anthropogenic sources (Schauer et al., 2001, 2002a, b), as well as being secondary products of atmospheric oxidation of hydrocarbons (Chacon-Madrid et al., 2010; Zhang et al., 2015; Han et al., 2016).

The most abundant atmospheric carbonyls are methanal (formaldehyde) and ethanal (acetaldehyde), and many studies have described their emission sources and chemical formation in urban and rural samples (Duan et al., 2016). Long-chain aliphatic carbonyl compounds have been identified in PM and reported in few published papers (Gogou et al., 1996; Andreou and Rapsomanikis, 2009), and these compounds are considered to be formed from atmospheric oxidation processes affecting biogenic emissions of alkanes. Anthropogenic activity is also considered to be a significant contributor to the aliphatic carbonyls. Appreciable concentrations of aliphatic carbonyl compounds have been identified in emissions from road vehicles (Schauer et al., 1999a; 2002b), coal combustion (Oros and Simoneit, 2000), wood burning (Rogge et al., 1998) and cooking processes (Zhao et al., 2007a,b), spanning a wide range of molecular weights. Furthermore, chamber studies (Chacon-Madrid and Donahue, 2011; Algrim and Ziemann, 2016) have demonstrated that the aliphatic carbonyl compounds are very important precursors of secondary organic aerosol (SOA) when they react with OH radicals in the presence of NO_x.

The oxidation of n-alkanes by hydroxyl radical is considered to be an important source of aliphatic carbonyl compounds. It was believed that the n-alkanals with carbon atoms numbering less than 20 indicate oxidation of alkanes, whereas the higher compounds were usually considered to be of direct biogenic origin (Rogge et al., 1998). The homologues and isomers of n-alkanals and n-alkanones have been identified as OH oxidation products of n-alkanes in many chamber and flow tube studies (Zhang et al., 2015; Schilling Fahnestock et al., 2015; Ruehl et al., 2013; Yee et al., 2012), although not all studies identified the position of the carbonyl group. The commonly accepted oxidation pathways of n-alkanes generally divide into functionalization and fragmentation. Functionalization occurs when an oxygenated functional group ($–ONO_2$, –OH, –C=O, –C(O)O– and –OOH) is added to a molecule, leaving the carbon skeleton intact. Alternatively, fragmentation involves C−C bond cleavage and produces two oxidation products with smaller carbon numbers than the reactant. The chamber studies of dodecane oxidation include observations of aldehydes and ketones as oxidation products (Schilling Fahnestock et al., 2015; Yee et al., 2012).

In London, with a high population density and a large number of diesel engine vehicles, the aliphatic hydrocarbons constitute an important fraction of ambient aerosols. Anthropogenic activities and secondary formation contribute to the emission and production of carbonyl compounds within the city. The objectives of the present study were the identification and quantification of aliphatic carbonyl compounds in particle and vapour samples collected in London from January to April 2017. This work has aided an understanding of the concentrations and secondary formation of carbonyls in the London atmosphere. Spatial and temporal variations of the studied carbonyl compounds were assessed and used to infer sources. One of the main objectives was to provide gas/particle partitioning

coefficients of identified carbonyls under realistic conditions. Diagnostic criteria were used to estimate the sources of identifiable atmospheric carbonyl compounds. Additionally, for the first time, concentrations of particulate and gaseous n-alkan-3-ones are reported.

2. MATERIALS AND METHODS

2.1 Sampling Method and Site Characteristics

Three sampling campaigns were carried out between 23 January and 18 April 2017 at four sampling sites (Figure 1) in London. The first campaign used two sampling sites, one located on the roof of a building (15 m above ground) of the Regent's University (51°31′N, -0°9′W), hereafter referred to as RU, sampled from 23 January 2017 to 19 February 2017, the other located on the roof (20 m above ground) of a building which belongs to the University of Westminster on the southern side of Marylebone Road (hereafter referred to as WM), sampled from 24 January 2017 to 20 February 2017. The third sampling site was located at ground level at Eltham (51°27′N, 0°4′E), hereafter referred to as EL, sampled from 23 February 2017 to 21 March 2017, which is located in suburban south London, and the fourth sampling site was located at ground level on the southern side of Marylebone Road (51°31′N, -0°9′W), hereafter referred to as MR, sampled from 22 March 2017 to 18 April 2017. Marylebone Road is in London's commercial centre, and is an important thoroughfare carrying 80-90,000 vehicles per day through central London. The Regent's University site is within Regent's Park to the north of Marylebone Road. The Eltham site is in a typical residential neighbourhood, 22 km from the MR site. Earlier work at the Marylebone Road and a separate Regent's Park site is described by Harrison et al. (2012).

The particle samples were collected on polypropylene backed PTFE filters (47 mm, Whatman) which preceded stainless steel sorbent tubes packed with 1cm quartz wool, 300 mg Carbograph 2TD 40/60 (Markes International, Llantrisant, UK) and sealed with stainless-steel caps before and after sampling. Sampling took place for sequential 24-hour periods at a flow rate of 1.5 L min^{-1} using an in-house developed automated sampler. Field blank filters and sorbent tubes were prepared for each site, and recovery efficiencies were evaluated. After the sampling, each filter was placed in a clean sealed petri dish, wrapped in aluminium foil and stored in the freezer at -18ºC prior to analysis. Black carbon (BC) was simultaneously monitored during the sampling period at RU and WM sites using an aethalometer (Model AE22, Magee Science). Measurements of BC and NO_x at MR and NO_x at EL were provided by the national network sites of Marylebone Road, and Eltham (https://uk-air.defra.gov.uk/).

2.2 Analytical Instrumentation

The particle samples were analyzed using a 2D gas chromatograph (GC, 7890A, Agilent Technologies, Wilmington, DE, USA) equipped with a Zoex ZX2 cryogenic modulator (Houston, TX, USA). The first dimension was equipped with a SGE DBX5, non-polar capillary column (30.0 m, 0.25 mm ID, 0.25 mm – 5.00% phenyl polysilphenylene-siloxane), and the second-dimension column equipped with a SGE DBX50 (4.00 m, 0.10 mm ID, 0.10 mm – 50.0% phenyl polysilphenylene-siloxane). The GC × GC was interfaced with a Bench-ToF-Select, time-of-flight mass spectrometer (ToF-MS, Markes International, Llantrisant, UK). The acquisition speed was 50.0 Hz with a mass resolution of >1200 fwhm at 70.0 eV and the mass range was 35.0 to 600 m/z. All data produced were processed using GC Image v2.5 (Zoex Corporation, Houston, US).

2.3 Analysis of Samples

Standards used in these experiments included 19 alkanes, C_8 to C_{26} (Sigma-Aldrich, UK, purity >99.2%); 12 n-aldehydes, C_8 to C_{13} (Sigma-Aldrich, UK, purity ≥95.0%), C_{14} to C_{18} (Tokyo Chemical Industry UK Ltd, purity >95.0%); and 10 2-ketones, C_8 to C_{13} and C_{15} to C_{18} (Sigma-Aldrich, UK, purity ≥98.0%) and C_{14} (Tokyo Chemical Industry UK Ltd, purity 97.0%).

The filters were spiked with 30.0 μL of 30.0 μg mL^{-1} deuterated internal standards (dodecane-d_{26}, pentadecane-d_{32}, eicosane-d_{42}, pentacosane-d_{52}, triacontane-d_{62}, butylbenzene-d_{14}, nonylbenzene-2,3,4,5,6-d_5, biphenyl-d_{10}, p-terphenyl-d_{14}; Sigma-Aldrich, UK) for quantification and then immersed in dichloromethane (DCM), and ultra-sonicated for 20.0 min at 20.0ºC. The extract was filtered using a clean glass pipette column packed with glass wool and anhydrous Na_2SO_4, and concentrated to 50.0 μL under a gentle flow of nitrogen for analysis using GC × GC-ToF-MS. 1 μL of the extracted sample was injected in a split ratio 100:1 at 300ºC. The initial temperature of the primary oven (80.0ºC) was held for 2.0 min and then increased at 2.0 ºC min^{-1} to 210ºC, followed by 1.5 ºC min^{-1} to 325 ºC. The initial temperature of the secondary oven (120ºC) was held for 2.0 min and then increased at 3.0ºC min^{-1} to 200ºC, followed by 2.00ºC min^{-1} to 300ºC and a final increase of 1.0ºC min^{-1} to 330 ºC to ensure all species passed through the column. The transfer line temperature was 330 ºC and the ion source temperature was 280ºC. Helium was used as the carrier gas at a constant flow rate of 1.0 mL min^{-1}. Further details of the instrumentation and data processing methods is given by Alam et al. (2016a,b).

156 The sorbent tubes were analyzed by an injection port thermal desorption unit (Unity 2, Markes
157 International, Llantrisant, UK) and subsequently analyzed using GC × GC-ToF-MS. Briefly, the
158 tubes were spiked with 1 ng of deuterated internal standard for quantification and desorbed onto the
159 cold trap at 350ºC for 15.0 min (trap held at 20.0ºC). The trap was then purged onto the column in
160 a split ratio of 100:1 at 350ºC and held for 4.0 min. The initial temperature of the primary oven
161 (90.0ºC) was held for 2.0 min and then increased to 2.0ºC min^{-1} to 240ºC, followed by 3.0ºC min^{-1}
162 to 310ºC and held for 5.0 min. The initial temperature of the secondary oven (40.0ºC) was held for
163 2.0 min and then increased at 3.0ºC min^{-1} to 250ºC, followed by an increase of 1.5ºC min^{-1} to 315ºC
164 and held for 5.0 min. Helium was used as carrier gas for the thermally desorbed organic compounds,
165 with a gas flow rate of 1.0 mL min^{-1}.

166

167 *Qualitative analysis*

168 Compound identification was based on the GC×GC-TOFMS spectra library, NIST mass spectral
169 library and in conjunction with authentic standards. Compounds within the homologous series for
170 which standards were not available were identified by comparing their retention time interval between
171 their homologues, and by comparison of mass spectra to the standards for similar compounds within
172 the series, by comparison to the NIST mass spectral library and by the analysis of fragmentation
173 patterns.

174

175 *Quantitative analysis*

176 An internal standard solution (outlined above) was added to the samples to extract prior to
177 instrumental analysis. Five internal standards (pentadecane-d_{32}, eicosane-d_{42}, pentacosane-d_{52},

178 triacontane-d_{62}, nonylbenzene-2,3,4,5,6-d_5) were used in the calculation of carbonyl compound
179 concentrations.
180
181 The quantification for alkanes, aldehydes and 2-ketones was performed by the linear regression
182 method using seven-point calibration curves (0.05, 0.10, 0.25, 0.50, 1.00, 2.00, 3.00 ng μL^{-1})
183 established between the authentic standards/internal standard concentration ratios and the
184 corresponding peak area ratios. The calibration curves for all target compounds were highly linear
185 (r^2>0.99, from 0.990 to 0.997), demonstrating the consistency and reproducibility of this method.
186 Limits of detection for individual compounds were typically in the range 0.04–0.12 ng m^{-3}. 3-ketones
187 were quantified using the calibration curves for 2-ketones. This applicability of quantification of
188 individual compounds using isomers of the same compound functionality (which have authentic
189 standards) has been discussed elsewhere and has a reported uncertainty of 24% (Alam et al., 2018).
190 Alkan-2-ones and alkan-3-ones were not well separated by the chromatography. These were separated
191 manually using the peak cutting tool, attributing fragments at m/z 58 and 71 to 2-ketones and m/z 72
192 and 85 to 3-ketones.
193
194 Field and laboratory blanks were routinely analysed to evaluate analytical bias and precision. Blank
195 levels of individual analytes were normally very low and in most cases not detectable. Recovery
196 efficiencies were determined by analyzing the blank samples spiked with standard compounds. Mean
197 recoveries ranged between 78.0 and 102%. All quantities reported here have been corrected according
198 to their recovery efficiencies.
199

3. RESULTS AND DISCUSSION

3.1 Mass Concentration of Particle-Bound Carbonyl Compounds

The study of temporal and spatial variations of air pollutants can provide valuable information about their sources and atmospheric processing. The time series of particle-bound n-alkanals, n-alkan-2-ones, and n-alkan-3-ones are plotted in Figure 2. It is clear that the concentrations of n-alkanals varied substantially with date, and were always higher than n-alkanones at four sites. It is also clear from Figure 3 that concentrations were broadly similar at the background sites, RU, WM and EL, but are elevated, especially for the n-alkanals, at MR. This is strongly indicative of a road traffic source.

Carbonyls including n-alkan-2-one and n-alkan-3-one homologues could result as fragmentation products from larger alkane precursors during gas-phase oxidation (Yee et al., 2012; Schilling Fahnestock et al., 2015) or as functionalized products from heterogeneous oxidation of particle-bound alkanes (Ruehl et al., 2013; Zhang et al., 2015). While carbonyl compounds are expected to be amongst first generation oxidation products of alkanes, product yields are not well known, and are highly dependent upon the chemical environment in which oxidation occurs. Yee et al. (2012) show substantial yields of mono-carbonyl product, the position of substitution undefined, in the low-NO_x oxidation of n-dodecane. Ruehl et al. (2013) report the production of 2- through 14-octacosanone from the oxidation of octacosane, giving relative, but not absolute yields. Schilling Fahnestock et al. (2014) report oxidation products of dodecane formed in both low-NO and high NO environments (<d.l and NO = 97.5 ppb respectively). A singly substituted unfragmented ketone product is reported only from the low-NO oxidation, and in relatively low yield amongst many products. Lim and Ziemann (2009) propose a reaction scheme for the OH-initiated oxidation of alkanes in the

222 presence of NO_x. They express the view that first generation carbonyl formation is negligible at
223 high NO concentrations for linear alkanes with C_n>6 since reactions of an alkylperoxy radical with
224 O_2 are to slow to compete with isomerisation, which leads ultimately to hydroxynitrate and
225 hydroxycarbonyl products. Ziemann (2011) also shows a substantial yield of alkylnitrates from OH-
226 initiated oxidation of n-alkanes from C_{10}-C_{25} in the presence of NO. The NO concentrations in the
227 background air of London are <12 ppb typically (UK-Air, 2018), and hence lie between the low and
228 high NO environments of experiments in the literature, therefore most probably permitting some
229 oxidation to proceed through pathways leading to first generation carbonyl products.

230

231 Figure 3 shows the average total concentrations of particle-bound 1-alkanals, n-alkan-2-ones, and
232 n-alkan-3-ones from January to April at four measurement sites, and the particle and gaseous phase
233 concentrations are detailed in the Table S1 (Supporting Information). Total n-alkanals was defined
234 as the sum of particle-bound n-alkanals ranging from C_8 to C_{20}. The particulate n-alkanals at the MR
235 site accounted for 75.2% of the measured particle carbonyls with the average total concentration of
236 682 ng m^{-3}, and concentrations at the other sites were 167 ng m^{-3} at EL, 117 ng m^{-3} at WM and 82.6
237 ng m^{-3} at RU, accounting for 57.0%, 57.9% and 56.3% of the measured particulate carbonyls,
238 respectively. The n-alkanals identified in this study differed substantially from those previously
239 reported in samples collected from Crete (Gogou et al., 1996) and Athens (Andreou and
240 Rapsomanikis, 2009) in Greece. The n-alkanals from London presented narrower ranges of carbon
241 numbers and a higher concentration than rural and urban samples from Crete. The concentrations of
242 n-alkanal homologues (C_8-C_{20}) ranged from 5.50 to 141 ng m^{-3} (average 52.0 ng m^{-3}) at MR which
243 were far higher than 1.48-28.6 ng m^{-3} (average 6.44 ng m^{-3}) at RU, 1.42-50.3 ng m^{-3} (average 9.03

244 ng m^{-3}) at WM and 3.29-53.0 ng m^{-3} (average 13.0 ng m^{-3}) at EL (Table S1), unlike Crete where the
245 concentrations were 0.9-3.7 ng m^{-3} in rural (C_{15}-C_{30}) and 5.4-6.7 ng m^{-3} in urban (C_9-C_{22}) samples,
246 and the average concentration of all four sites was much higher than the 0.91 ng m^{-3} measured in
247 Athens (Andreou and Rapsomanikis, 2009) (C_{13}-C_{20}). This is a clear indication of a road traffic,
248 most probably diesel source which is greater in London.

249

250 As part of the CARBOSOL project (Oliveira et al., 2007), air samples were collected in summer and
251 winter at six rural sites across Europe. The particulate n-alkanals ranged from C_{11} to C_{30} with average
252 total concentrations between 1.0 ng m^{-3} and 19.0 ng m^{-3}, with higher concentrations in summer than
253 winter at all but one site. Maximum concentrations at all sites were in compounds >C_{22} indicating a
254 source from leaf surface abrasion products and biomass burning (Simoneit et al., 1967; Gogou et al.,
255 1996). This far exceeds the C_{max} values seen in the particulate fraction at our sites.

256

257 The n-alkan-2-one homologues measured in London ranged from C_8 to C_{26}, and the average total
258 particulate fraction concentration was 58.5 ng m^{-3} at RU, 75.1 ng m^{-3} at WM, 112 ng m^{-3} at EL and
259 186 ng m^{-3} at MR, approximately accounting for 39.9% (RU), 37.0% (WM), 38.1% (EL) and 20.5%
260 (MR) of the total particulate carbonyls, respectively (Figure 3). The published data from Greece
261 indicated that the concentrations of n-alkan-2-ones were independent of the seasons, and an average
262 of 5.40 ng m^{-3} (C_{13}-C_{29}) was measured in August and 5.44 ng m^{-3} in March at Athinas St, but 12.88
263 ng m^{-3} was measured in March at the elevated (20 m) AEDA site in Athens (Gogou et al., 1996).
264 Concentrations in Crete for alkan-2-ones (C_{10}-C_{31}) were 0.4-2.1 ng m^{-3} at the rural site and 1.9-2.6
265 ng m^{-3} at the urban site (Andreou and Rapsomanikis, 2009). The CARBOSOL project also

266 determined concentrations of n-alkan-2-ones, between C_{14} and C_{31} with a C_{max} at C_{28} or C_{29} at all
267 but one site. Average concentrations ranged from 0.15 ng m^{-3} (C_{17-29}) to 3.35 (C_{14}-C_{31}), very much
268 below the concentrations at our London sampling site. Cheng et al. (2006) measured concentrations
269 of n-alkan-2-ones in the Lower Fraser Valley, Canada, in $PM_{2.5}$. Samples collected in a road tunnel
270 showed the highest concentrations, total 1.8-12.6 ng m^{-3} for C_{10}-C_{31}, and were higher in daytime
271 than nighttime. Concentrations at a forest site were 1.1-7.2 ng m^{-3} without a diurnal pattern. Values
272 of C_{max} ranged from C_{16-17} at the road tunnel to C_{27} (secondary maximum) at the forest site. Values
273 of CPI averaged across sites from 1.00 to 1.34, giving little evidence for a substantial biogenic input
274 from higher plant waxes. These data clearly suggest a road traffic source in London, but less
275 influential than for the n-alkanals for which the increment at the roadside MR site is much greater.
276
277 The n-alkan-3-one homologues identified in the samples ranged from C_8 to C_{19}, and the average of
278 individual compound concentrations was 0.52 ng m^{-3} at RU, 0.94 ng m^{-3} at WM, 1.37 ng m^{-3} at EL
279 and 3.34 ng m^{-3} at MR. The concentrations of n-alkan-3-ones at the four sites were lower than the n-
280 alkanals and n-alkan-2-ones, and MR had the highest average total mass concentrations 39.4 ng m^{-3},
281 followed by 14.3 ng m^{-3} at EL, 10.4 ng m^{-3} at WM and 5.65 ng m^{-3} at RU, respectively.
282
283 The isomeric carbonyls formed via OH-initiated heterogeneous reactions of n-octacosane (C_{28})
284 exhibit a pronounced preference at the 2-position of the molecule chain (Ruehl et al., 2013). The n-
285 octacosan-2-ones have the highest relative yield (1.00), followed by n-octacosan-3-ones (0.50), while
286 other isomeric carbonyl yields were lower than 0.20. The same results were found in the subsequent
287 chamber studies of n-alkanes (Zhang et al., 2015) (C_{20}, C_{22}, C_{24} but not C_{18}). The main probable

288 reason was that a large fraction of C_{18} evaporated into the gas phase, and OH oxidation happened in
289 the gas phase (homogeneous reaction). This may be supported by the evidence from previous studies
290 (Kwok and Atkinson, 1995; Ruehl et al., 2013), which found that the isomeric distribution of
291 oxidation products of n-alkanes depends upon whether the reaction occurs in the gas phase or at the
292 particle surface (Kwok and Atkinson, 1995; Ruehl et al., 2013). The homogeneous gas-phase
293 oxidation occurs fast, and H-abstraction by OH radicals occurs at all carbon sites. The fractions of
294 the OH radical reaction by H atom abstraction from n-decane at the 1-, 2-, 3-, 4- and 5-positions are
295 3.10%, 20.7%, 25.4%, 25.4%, and 25.4%, respectively, and the products from gas phase
296 (homogeneous) reaction were generally in accord with structure-reactivity relationship (SRR)
297 predictions (Kwok and Atkinson, 1995; Aschmann et al., 2001). Zhang et al. (2015) report on the
298 competition between homogeneous and heterogeneous oxidation of medium to high molecular weight
299 alkanes. They express the view that in the atmosphere, compounds typically classified as semi-
300 volatile evaporate sufficiently rapidly that homogeneous gas phase oxidation is more rapid than
301 oxidation in the condensed phase.
302
303 During the field experiment, the n-alkanal homologues were abundant in all samples, and this is
304 probably attributable to the primary emission sources, including diesel vehicles (Schauer et al.,
305 1999a), gasoline cars (Schauer et al., 2002b), wood burning (Rogge et al., 1998) and cooking aerosol
306 (Schauer et al., 1999b). Correlations with other largely vehicle-generated pollutants (see later)
307 support this interpretation. The particulate form of the n-alkane homologues (C_{14}-C_{36}) identified in
308 the samples dominated for $>C_{25}$ and there was a significant particulate fraction for all but the low
309 MW n-alkanes (unpublished data). The H-abstraction by OH radicals may therefore have been

310 dominated by heterogeneous reactions generating the higher concentrations of n-alkan-2-ones than
311 n-alkan-3-ones that were found in all samples. The ratio of n-alkan-2-ones/n-alkan-3-ones (C_{11}-C_{18})
312 with the same carbon atom number ranged from 2.35-11.3 at four measurement sites. Surprisingly,
313 although the n-alkane (C_{11}-C_{13}) oxidation was expected to be dominated by homogeneous gas phase
314 reactions, the n-alkan-2-one/n-alkan-3-one ratios were still greater than 2.00. The probable reason
315 was that the lower molecular weight n-alkan-2-ones were significantly impacted by primary emission
316 sources such as cooking (Zhao et al., 2007a,b). Another likely reason is that the n-alkan-2-one and n-
317 alkan-3-one homologues with lower carbon atom numbers originated in part from the fragmental
318 products of higher n-alkanes (Yee et al., 2012; Schilling Fahnestock et al., 2015).
319
320 The ratios of n-alkan-2-ones/n-alkanes, n-alkan-3-ones/n-alkanes (with same carbon numbers) were
321 calculated and are reported in Table S2. The n-alkan-3-ones with carbon numbers higher than C_{20}
322 were not identified in the samples, indicating that both the gas phase and heterogeneous reactions of
323 higher molecular weight n-alkanes were slow, the former probably due to the low vapour phase
324 presence of n-alkanes. The ratios of n-alkan-3-ones/n-alkanes at four measurement sites gradually
325 increased from $C_{11,}$ and then decreased from C_{17}, while higher ratios of n-alkan-2-ones/n-alkanes were
326 observed in the range from C_{17} to C_{22}, probably indicating a shift from homogeneous reactions to
327 heterogeneous reactions with the increase of carbon numbers. The low ratios of n-alkan-2-ones/n-
328 alkanes with carbon numbers from C_{23} to C_{26} might be explained by the low diffusion rate from the
329 inner particle to the surface with the increasing carbon number of n-alkanes, even though
330 heterogeneous reactions would be the expected dominant pathway.
331

3.2 Sources of Carbonyl Compounds

3.2.1 Homologue distribution and carbon preference index (CPI)

Figure 4 shows the average concentrations, and molecular distributions of particle-bound carbonyl compounds at the four sites. The values of carbon preference index (CPI) were calculated to estimate the origin of carbonyl compounds, according to Bray and Evans (1961):

$$\mathrm{CPI} = \frac{1}{2}\left(\frac{\sum_4^m C_{2i+1}}{\sum_4^m C_{2i}} + \frac{\sum_4^m C_{2i+1}}{\sum_5^{m+1} C_{2i}}\right)$$

For n-alkanals and n-alkan-3-ones (m=9): $\mathrm{CPI} = \frac{1}{2}\left(\frac{\sum odd(C_9-C_{19})}{\sum even(C_8-C_{18})} + \frac{\sum odd(C_9-C_{19})}{\sum even(C_{10}-C_{20})}\right)$

For n-alkan-2-ones (m=12): $\mathrm{CPI} = \frac{1}{2}\left(\frac{\sum odd(C_9-C_{25})}{\sum even(C_8-C_{24})} + \frac{\sum odd(C_9-C_{25})}{\sum even(C_{10}-C_{26})}\right)$

where *i* takes values between 4 and *m*, and 5 and *m* as in the equation, and

m = 9 for n-alkanal and n-alkan-3-ones

m = 12 for n-alkan-2-ones

The carbon number of the homologue of highest concentration (C_{max}) can be indicative of the source. Table. 1 presents the CPI and C_{max} of particle-bound carbonyl compounds calculated in the current and other studies. A CPI of ≤1 is an indication of an anthropogenic source, while a CPI of 1-5 shows a mixture of anthropogenic and biogenic sources and a CPI >5 suggests a biogenic (plant wax) source.

352 The n-alkanes which are potential precursors of the oxygenates described typically showed two C_{max}
353 values, the first at C_{13} (the lowest MW compound measured), and at C_{23}. The CPI values for the
354 n-alkanes were between 0.97-1.02 at the four measurements sites (unpublished data).

355

356 According to the low CPI (0.41-1.07) at the four sites, the n-alkanal homologues with carbon number
357 from C_8 to C_{20} mainly originate from anthropogenic emissions or OH oxidation of fossil-derived
358 hydrocarbons. The particle-bound n-alkanals exhibited a similar distribution of carbon number from
359 January to April at four sites, and they had the same C_{max} at C_8 with concentration 28.6 ng m^{-3} at
360 RU, 50.3 ng m^{-3} at WM, 53.0 ng m^{-3} at EL and 141 ng m^{-3} at MR, respectively. This compound may
361 be a fragmentation product, oxidation product or primary emission. In addition, the distribution of
362 n-alkanals had a second concentration peak at C_{15} (MR) and C_{18} (RU, WM, and EL). The C_{18}
363 compound was observed accounting for the highest percentage of the total mass of n-alkanals in
364 some rural aerosol samples (Gogou et al., 1996) in Crete. Andreou and Rapsomanikis reported the
365 C_{max} as C_{15} or C_{17} in Athens (Andreou and Rapsomanikis, 2009) and attributed this to the oxidation
366 of n-alkanes. However, a C_{max} at C_{26} or C_{28} in urban Crete (Gogou et al., 1996) was observed,
367 suggestive of biogenic input. The homologue distribution and CPI of n-alkanals in this study differed
368 from those previous reports, and demonstrated weak biogenic input and a strong impact of
369 anthropogenic activities in the London samples.

370 In this study, n-alkan-2-ones have similar homologue distributions and C_{max} (C_{19} or C_{20}) (Table 2)
371 at RU, WM and EL sites, and the total concentration from C_{16} to C_{23} accounts for 76.0%, 76.1% and
372 68.0% of ∑n-alkan-2-ones, respectively. The CPI values for n-alkan-2-ones ranged from 0.57 to
373 1.23 at the RU, MR and WM sites and were not indicative of major biogenic input, and were

374 considered to mainly originate from anthropogenic activities and OH oxidation of anthropogenic n-
375 alkanes. It is however notable that the CPI values for both the 2-ketones and 3-ketones exceed
376 those for the alkanals (see Table 1), suggesting a contribution from contemporary biogenic sources,
377 possibly wood smoke and cooking. At EL, the CPI of 1.57 is clearly indicative of a biogenic
378 contribution in suburban south London. A difference was observed at the MR site, the n-alkan-2-
379 ones with carbon atoms numbering from C_{12} to C_{18} accounting for 72.0% of ∑n-alkan-2-ones, with
380 the C_{max} being at C_{16}. These data suggest a contribution of primary emissions from traffic at MR,
381 but a dominant background, probably substantially secondary, at the other sites. The C_{max} of n-alkan-
382 3-ones was at C_{16} at the MR site, at EL, $C_{max} = C_{16}$, WM, $C_{max} = C_{17}$ and at RU, $C_{max} = C_{17}$,
383 respectively.

384

385 **3.2.2 The ratios of n-alkanes/n-alkanals**

386 Diesel engine emission studies have been conducted previously in our group; details of the engine set
387 up and exhaust sampling system are given elsewhere (Alam et al., 2016b). Briefly, the steady-state
388 diesel engine operating conditions were at a load of 5.90 bar mean effective pressure (BMEP) and a
389 speed of 1800 revolutions per minute (RPM), and samples (n=14) were collected both before a diesel
390 oxidation catalyst (DOC) and after a diesel particulate filter (DPF). The n-alkanes (C_{12} - C_{37}) and 1-
391 alkanals (C_9 - C_{18}) were quantified in the particle samples, while n-alkanones were not identified
392 because their concentrations were lower than the limits of (detection 0.01–0.15 ng m^{-3}). The emission
393 concentrations of n-alkanals ranged from 7.10 to 53.2 µg m^{-3} (before DOC) and 1.20 to 11.5 µg m^{-3}
394 (after DPF), respectively, and the ratios of alkanes/alkanals (C_{13}-C_{18}) with the same carbon atom
395 numbers ranged from 0.15 to 0.23 (before DOC) and 0.52 to 7.60 (after DPF). The n-alkane/n-alkanal

(C_{13}-C_{18}) ratio at MR ranged from 0.30 to 5.7, while average ratios of 14.9 (RU), 11.5 (WM) and 14.7 (EL) were obtained, respectively. The similarity of the n-alkanes/n-alkanal ratio between MR and the engine studies (after DPF) strongly suggests that diesel vehicle emissions were the main source of alkanals at MR. The higher ratios at the other sites may be due to greater airmass aging and loss of alkanals due to their higher reactivity (Chacon-Madrid and Donahue, 2011; Chacon-Madrid et al., 2010).

The emission factors of total alkanes from diesel engines are reported to be 7 times greater than gasoline engines (Perrone et al., 2014), with n-alkanals with carbon atoms numbering lower than C_{11} being quantified in the exhaust from gasoline engines (Schauer et al., 2002b; Gentner et al., 2013). The n-alkane/n-alkanal (C_8-C_{10}) ratio with the same carbon numbers ranged from 5.60 to 14.3 (Schauer et al., 2002b), suggesting that gasoline combustion may be another potential source of atmospheric n-alkanals.

3.2.3 Correlation analysis

Insights into the sources of carbonyls can be gained from intra-site correlation analysis with black carbon (BC) and NO_x. This is more informative than comparisons between sites when sampling did not take place simultaneously, as concentrations are strongly affected by weather conditions, making inter-site comparisons difficult to interpret. In London, both black carbon and NO_x arise very substantially from diesel vehicle emissions (Liu et al., 2014; Harrison et al., 2012; Harrison and Beddows, 2017), and hence these are good measures of road traffic activity. The concentrations of BC were simultaneously determined by the online instruments during the sampling periods, with the

418 average concentrations of 1.34, 1.94 and 3.58 μg m^{-3} at the RU, WM and MR sites, respectively.
419 The data for NO_x were provided by the national network sites, with the average concentrations of
420 23.4 and 202 μg m^{-3} at the EL and MR sites, respectively. At the MR site, the concentrations of BC
421 and NO_x averaged 5.00 μg m^{-3} and 281 μg m^{-3} when southerly winds were dominant compared to
422 2.60 and 128 μg m^{-3} for northerly winds. All correlations were carried out with the sum of particle
423 and vapour phases for the carbonyl compounds, and strong (r^2 = 0.87) and weak (r^2 = 0.12)
424 correlations between BC and NO_x were obtained when the southerly and northerly winds were
425 prevalent at MR, respectively. Marylebone Road is a street canyon site where a vortex circulation is
426 established by the wind. The effect is that on northerly wind sectors the sampling site on the southern
427 side of the road samples near-background air, while on southerly wind sectors, the traffic pollution
428 is carried to the sampling site, leading to elevated pollution levels affected heavily by the traffic
429 emissions. The strong correlation between BC and NO_x with southerly wind sectors is a reflection
430 of their emission from road traffic. In addition, the correlations between n-alkanals (C_8-C_{20}) and BC,
431 and between n-alkanals (C_8-C_{20}) and NO_x were calculated to assess the contribution of vehicular
432 emissions (Table S3). The results showed that the correlations (r^2) between n-alkanals and BC
433 gradually decreased from 0.61 (C_9) to 0.34 (C_{20}) at MR when the southerly winds were prevalent,
434 indicating that the distribution of n-alkanals, and especially the lower MW compounds, was
435 significantly impacted by the vehicular exhaust emissions. The average correlations at MR
436 (southerly winds) between n-alkanals and BC, and between n-alkanals and NO_x were r^2 = 0.47 and
437 r^2 = 0.32, respectively. These moderate correlations demonstrated that the vehicular emissions were
438 a source of n-alkanals at MR, and contribute to the high background concentrations of n-alkanals in
439 London. The other probable sources of n-alkanals include cooking emissions, wood burning,

440 photooxidation of hydrocarbons and industrial emissions. Poorer correlations between n-alkanals
441 and BC (average $r^2 = 0.15$), and between n-alkanals and NO_x (average $r^2 = 0.15$) were observed at
442 MR in the north London background air sampled when northerly winds were prevalent. There were
443 very weak correlations (average $r^2 < 0.10$) between n-alkanals and BC, and between n-alkanals and
444 NO_x at the RU, WM and EL sites, which may be attributable to the high chemical reactivity of n-
445 alkanals. High concentrations of furanones (γ-lactones) are generated via the photo-oxidation
446 reaction of n-alkanals (Alves et al., 2001), and the total concentrations (particle and gas) were up to
447 376, 279, 347 and 318 ng m^{-3} at RU, WM, WL, and MR, respectively for the sum of furanone
448 homologues (from 5-propyldihydro-2(3H)-furanone to 5-tetradecyldihydro-2(3H)-furanone).

449

450 The relationships (r^2 values) between BC and NO_x and the n-alkan-2-ones were low at all sites, but
451 notably higher with southerly winds at MR (average $r^2 = 0.33$ and 0.35 for BC and NO_x respectively)
452 than for northerly winds ($r^2 = 0.16$ and 0.03 respectively). This is strongly suggestive of a
453 contribution from vehicle exhaust to n-alkan-2-one concentrations, but smaller than that for n-
454 alkanals. In the case of the n-alkan-3-ones, correlations averaged $r^2 = 0.25$ with BC and $r^2 = 0.21$ for
455 NO_x in southerly winds, compared to $r^2 = 0.08$ and $r^2 = 0.05$ respectively for northerly winds. This
456 is also suggestive of a small, but not negligible contribution of vehicle emissions to n-alkan-3-ones.
457 The very low correlations observed in background air for both n-alkan-2-ones and n-alkan-3-ones
458 with BC and NO_x are suggestive of the importance of non-traffic sources, probably including
459 oxidation of n-alkanes. Both compound groups were below detection limit in the analyses of diesel
460 exhaust. The considerable predominance of n-alkan-2-one over n-alkan-3-one concentrations may

be indicative of a formation pathway from oxidation of condensed phase n-alkanes, but this is speculative as primary emissions may be dominant.

3.3 Gas and Particle Phase Partitioning

The partitioning coefficient K_p between particles and vapour was calculated in this study according to the following equation defined by Pankow (1994):

$$K_p = \frac{C_p}{C_g * TSP}$$

Where, C_p and C_g (μg m^{-3}) are the concentration of the compounds in the particulate phase and gaseous phase, respectively. TSP is the concentration of total suspended particulate matter (μg m^{-3}), which was estimated from the PM_{10} concentration (PM_{10}/TSP = 0.80), and daily average PM_{10} concentrations were taken from the national network sites (see Table S5). The partitioning coefficients K_p calculated from our data and the percentages in the particulate form are presented in Table 2. For the three types of carbonyls, the n-alkanals >C_{16}, n-alkan-2-ones >C_{19}, and n-alkan-3-ones > C_{18} the vapour concentrations were below detection limit, and the partitioning into the particulate phase gradually increased from C_8 to high molecular weight compounds.

Log Kp was regressed against vapour pressure (VP_T) for the relevant temperature derived from UManSysProp (http://umansysprop.seaes.manchester.ac.uk/) according to the following equation:

$$\text{Log } K_p = \text{m} \log(VP_T) + b$$

The calculated log K_p versus log (VP_T) for the three types of carbonyls was calculated for each day, and the results appear in the Table S4. Data from four sites were over the temperature range 0.40–15.3 °C. A good fit to the data for n-alkan-2-ones (r^2 = 0.54–0.94 at RU, 0.64-0.93 at WM, 0.43-0.95 EL and 0.45-0.89 at MR) was obtained. It is notable that the fit to the regression equation as indicated by the r^2 value is appreciably higher at the MR site than at the other sites, especially in the case of the alkan-3-ones. This is not easily explained, except perhaps by an increased particle surface area at the MR site which may enhance the kinetics of gas-particle exchange, leading to partitioning which is closer to equilibrium.

4. CONCLUSIONS

Three groups of carbonyl compounds were determined in the particle and gaseous phase in London and concentrations are reported for n-alkanals (C_8-C_{20}), n-alkan-2-ones (C_8-C_{26}) and n-alkan-3-ones (C_8-C_{19}). The Marylebone Road site has the highest concentration of particle-bound n-alkanals, and the average total concentration was up to 682 ng m^{-3}, followed by 167 ng m^{-3} at EL, 117 ng m^{-3} at WM and 82.6 ng m^{-3} at RU. The particulate n-alkanals were abundant in all samples at all four measurement sites, accounting for more than 56.3% of total particle carbonyls. In addition, the average total particle concentrations of n-alkan-2-ones and n-alkan-3-ones at four measurement sites were in the range of 58.5-186 ng m^{-3} and 5.65-39.4 ng m^{-3}, respectively. Diagnostic criteria, including molecular distribution, CPI, C_{max}, ratios and correlations, were used to assess the sources and their contributions to carbonyl compounds. The three groups of carbonyls have similar molecular distributions and C_{max} values at the four measurement sites, and their low CPI values

505 (0.41-1.57) at the four sites indicate a weak biogenic input during sampling campaigns. Heavily
506 traffic-influenced air and urban background air were measured at the MR site when southerly and
507 northerly winds were prevalent respectively; correlations of r^2 = 0.47 and r^2=0.32 were obtained
508 between n-alkanals and BC, and between between n-alkanals and NO_x, respectively in southerly
509 winds. Vehicle emissions appear to be an important source of n-alkanals, which is confirmed by the
510 similar ratios of n-alkanes/n-alkanals measured at MR (0.30-5.75) and in diesel engine exhaust
511 studies (0.52-7.6), resulting in a high background concentration in London. In addition, the OH-
512 initiated heterogeneous reactions of n-alkanes appear to be important sources of n-alkanones, even
513 though weak contributions from vehicular exhaust emissions were suggested by correlation analysis
514 with BC and NO_x in southerly winds at MR. Anthropogenic primary sources such as cooking
515 (Abdullahi et al., 2013) may account for a proportion of the alkan-2-one and alkan-3-one
516 concentrations measured in London, in addition to the secondary contribution from alkane oxidation.
517 Any contribution from cooking or wood combustion is likely to be small, or the CPI would be greater.
518
519 In addition, the partitioning coefficients of carbonyls were determined from the relative proportions
520 of the particle and gaseous phases of individual compounds. The results of field measurements of
521 partitioning between particle and vapour phases showed generally a better fit at MR than at the other
522 three sites. The n-alkan-2-ones have a better fit at four sites than the n-alkanals and n-alkan-3-ones,
523 with r^2 = 0.72 (0.49–0.57) at RU, 0.76 (0.55-0.87) at WM, 0.74 (0.43-0.95) EL and 0.70 (0.45-0.89)
524 at MR, respectively in a regression of log K_p versus the compound vapour pressure. This most
525 likely reflects the slow formation of the alkan-2-ones as secondary constituents, closer to phase
526 equilibrium than the largely emitted alkanals which would be spatially far more variable. The

527 higher r^2 values for the alkan-2-ones than alkan-3-ones may reflect the higher concentrations, and
528 hence better analytical precision for the former compound group.
529
530 **ACKNOWLEDGEMENTS**
531 Primary collection of samples took place during the FASTER project which was funded by the
532 European Research Council (ERC-2012-AdG, Proposal No. 320821). The authors would also like
533 to thank the China Scholarship Council (CSC) for support to R.L., and the Natural Environment
534 Research Council for support under the Air Pollution and Human Health (APHH) programme
535 (NE/N007190/1).

REFERENCE

Abdullahi, K.L., Delgado-Saborit, J.M., and R.M. Harrison: Emissions and indoor concentrations of particulate matter and its specific chemical components from cooking: A review, Atmos. Environ., 71, 260-294, http://dx.doi.org/10.1016/j.atmosenv.2013.01.061, 2013.

Alam, M. S., Stark, C., and Harrison, R. M.: Using variable ionization energy time-of-flight mass spectrometry with comprehensive GC×GC to identify isomeric species, Anal. Chem., 88, 4211-4220, http://www.doi.org/10.1021/acs.analchem.5b03122, 2016a.

Alam, M. S., Zeraati-Rezaei, S., Stark, C. P., Liang, Z., Xu, H., and Harrison, R. M.: The characterisation of diesel exhaust particles - composition, size distribution and partitioning, Faraday. Discuss., 189, 69-84, http://www.doi.org/10.1039/C5FD00185D, 2016b.

Alam, M. S., Zeraati-Rezaei, S., Liang, Z., Stark, C., Xu, H., MacKenzie, A. R., and Harrison, R. M.: Mapping and quantifying isomer sets of hydrocarbons (≥ C 12) in diesel exhaust, lubricating oil and diesel fuel samples using GC× GC-ToF-MS, Atmos. Meas. Tech., 11, 3047, https://doi.org/10.5194/amt-11-3047-2018, 2018.

Algrim, L. B., and Ziemann, P. J.: Effect of the Keto Group on yields and composition of organic aerosol formed from OH radical-initiated reactions of ketones in the presence of NO_x, J. Phys. Chem. A., 120, 6978-6989, http://www.doi.org/10.1021/acs.jpca.6b05839, 2016.

Alves, C., Pio, C., and Duarte, A.: Composition of extractable organic matter of air particles from rural and urban Portuguese areas, Atmos. Environ., 35, 5485-5496, https://doi.org/10.1016/S1352-2310(01)00243-6, 2001.

Andreou, G., and Rapsomanikis, S.: Origins of n-alkanes, carbonyl compounds and molecular biomarkers in atmospheric fine and coarse particles of Athens, Greece, Sci. Total. Environ., 407, 5750-5760, http://dx.doi.org/10.1016/j.scitotenv.2009.07.019, 2009.

Aschmann, S. M., Arey, J., and Atkinson, R.: Atmospheric chemistry of three C10 alkanes, J. Phys. Chem. A., 105, 7598-7606, http://www.doi.org/10.1021/jp010909j, 2001.

Bray, E., and Evans, E.: Distribution of n-paraffins as a clue to recognition of source beds, Geochim. Cosmochim. Ac., 22, 2-15, https://doi.org/10.1016/0016-7037(61)90069-2, 1961.

Chacon-Madrid, H., and Donahue, N.: Fragmentation vs. functionalization: chemical aging and organic aerosol formation, Atmos. Chem. Phys., 11, 10553-10563, https://doi.org/10.5194/acp-11-10553-2011, 2011.

Chacon-Madrid, H. J., Presto, A. A., and Donahue, N. M.: Functionalization vs. fragmentation: n-aldehyde oxidation mechanisms and secondary organic aerosol formation, Phys. Chem. Chem. Phys., 12, 13975-13982, http://www.doi.org/10.1039/C0CP00200C, 2010.

Cheng, Y., Li, S.-M., Leithead, A., and Brook, J. R.: Spatial and diurnal distributions of n-alkanes and n-alkan-2-ones on PM 2.5 aerosols in the Lower Fraser Valley, Canada, Atmos. Environ., 40, 2706-2720, https://doi.org/10.1016/j.atmosenv.2005.11.066, 2006.

Duan, H., Liu, X., Yan, M., Wu, Y., and Liu, Z.: Characteristics of carbonyls and volatile organic compounds (VOCs) in residences in Beijing, China, Front. Env. Sci. Eng., 10, 73-84, http://www.doi.org/10.1007/s11783-014-0743-0, 2016.

Gentner, D. R., Worton, D. R., Isaacman, G., Davis, L. C., Dallmann, T. R., Wood, E. C., Herndon, S. C., Goldstein, A. H., and Harley, R. A.: Chemical composition of gas-phase organic carbon emissions from motor vehicles and implications for ozone production, Environ. Sci. technol., 47, 11837-11848, http://www.doi.org/10.1021/es401470e, 2013.

Gogou, A., Stratigakis, N., Kanakidou, M., and Stephanou, E. G.: Organic aerosols in Eastern Mediterranean: components source reconciliation by using molecular markers and atmospheric back trajectories, Org. Geochem., 25, 79-96, https://doi.org/10.1016/S0146-6380(96)00105-2, 1996.

Han, Y., Kawamura, K., Chen, Q., and Mochida, M.: Formation of high-molecular-weight compounds via the heterogeneous reactions of gaseous C8–C10 n-aldehydes in the presence of atmospheric aerosol components, Atmos. Environ., 126, 290-297, http://dx.doi.org/10.1016/j.atmosenv.2015.11.050, 2016.

Harrison, R., Dall'Osto, M., Beddows, D., Thorpe, A., Bloss, W., Allan, J., Coe, H., Dorsey, J., Gallagher, M., and Martin, C.: Atmospheric chemistry and physics in the atmosphere of a developed megacity (London): an overview of the REPARTEE experiment and its conclusions, Atmos. Chem. Phys., 12, 3065-3114, https://doi.org/10.5194/acp-12-3065-2012, 2012.

Harrison, R. M., and Beddows, D. C.: Efficacy of recent emissions controls on road vehicles in Europe and implications for public health, Sci. Rep-UK., 7, 1152, http://www.doi.org/10.1038/s41598-017-01135-2., 2017.

Kwok, E. S., and Atkinson, R.: Estimation of hydroxyl radical reaction rate constants for gas-phase organic compounds using a structure-reactivity relationship: an update, Atmos. Environ., 29, 1685-1695, https://doi.org/10.1016/1352-2310(95)00069-B, 1995.

Lim, Y. B., and Ziemann, P.J.: Chemistry of secondary organic aerosol formation from OH radical-initiated reactions of linear, branched, and cyclic alkanes in the presence of NO_x, Aerosol Sci. Technol., 43, 604-619, https://doi.org/10.1080/02786820902802567, 2009.

Liu, D., Allan, J., Young, D., Coe, H., Beddows, D., Fleming, Z., Flynn, M., Gallagher, M., Harrison, R., and Lee, J.: Size distribution, mixing state and source apportionments of black carbon aerosols in London during winter time, Atmos. Chem. Phys., 14, https://doi.org/10.5194/acp-14-10061-2014, 2014.

Oliveira, T. S., Pio, C., Alves, C. A., Silvestre, A. J., Evtyugina, M., Afonso, J., Fialho, P., Legrand, M., Puxbaum, H., and Gelencsér, A.: Seasonal variation of particulate lipophilic organic compounds at nonurban sites in Europe, J. Geophys. Res-Atmos., 112, https://doi.org/10.1029/2007JD008504 2007.

Oros, D. R., and Simoneit, B. R. T.: Identification and emission rates of molecular tracers in coal smoke particulate matter, Fuel., 79, 515-536, http://dx.doi.org/10.1016/S0016-2361(99)00153-2, 2000.

Pankow, J. F.: An absorption model of gas/particle partitioning of organic compounds in the atmosphere, Atmos. Environ., 28, 185-188, https://doi.org/10.1016/1352-2310(94)90093-0, 1994.

Perrone, M. G., Carbone, C., Faedo, D., Ferrero, L., Maggioni, A., Sangiorgi, G., and Bolzacchini, E.: Exhaust emissions of polycyclic aromatic hydrocarbons, n-alkanes and phenols from vehicles coming within different European classes, Atmos. Environ., 82, 391-400, https://doi.org/10.1016/j.atmosenv.2013.10.040, 2014.

Rogge, W. F., Hildemann, L. M., Mazurek, M. A., and Cass, G. R.: Sources of fine organic aerosol. 9. Pine, oak, and synthetic log combustion in residential fireplaces, Environ. Sci. Technol., 32, 13-22, http://www.doi.org/10.1021/es960930b, 1998.

Ruehl, C. R., Nah, T., Isaacman, G., Worton, D. R., Chan, A. W. H., Kolesar, K. R., Cappa, C. D., Goldstein, A. H., and Wilson, K. R.: The influence of molecular structure and aerosol phase on the heterogeneous oxidation of normal and branched alkanes by OH, J. Phys. Chem. A., 117, 3990-4000, http://www.doi.org/10.1021/jp401888q, 2013.

Schauer, J. J., Kleemanm M. J., Cass, G. R., and Simoneit, B. R. T.: Measurement of emissions from air pollution sources. 2. C1 through C30 organic compounds from medium duty diesel trucks, Environ. Sci.Technol., 33, 1578-1587, 10.1021/es980081n, 1999a.

Schauer, J. J., Kleeman, M. J., Cass, G. R., and Simoneit, B. R. T.: Measurement of emissions from air pollution sources. 1. C1 through C29 organic compounds from meat charbroiling, Environ. Sci. Technol., 33, 1566-1577, http://www.doi.org/10.1021/es980076j, 1999b.

Schauer, J. J., Kleeman, M. J., Cass, G. R., and Simoneit, B. R. T.: Measurement of emissions from air pollution sources. 3. C1−C29 organic compounds from fireplace combustion of wood, Environ. Sci. technol., 35, 1716-1728, http://www.doi.org/10.1021/es001331e, 2001.

Schauer, J. J., Kleeman, M. J., Cass, G. R., and Simoneit, B. R. T.: Measurement of emissions from air pollution sources. 4. C1−C27 organic compounds from cooking with seed oils, Environ. Sci. Technol., 36, 567-575, http://www.doi.org/10.1021/es002053m, 2002a.

Schauer, J. J., Kleeman, M. J., Cass, G. R., and Simoneit, B. R. T.: Measurement of emissions from air pollution sources. 5. C1−C32 organic compounds from gasoline-powered motor vehicles, Environ. Sci. Technol., 36, 1169-1180, http://www.doi.org/10.1021/es0108077, 2002b.

669
670 Schilling Fahnestock, K. A., Yee, L. D., Loza, C. L., Coggon, M. M., Schwantes, R., Zhang, X.,
671 Dalleska, N. F., and Seinfeld, J. H.: Secondary organic aerosol composition from C12 alkanes, J.
672 Phys. Chem. A., 119, 4281-4297, http://www.doi.org/10.1021/jp501779w, 2015.
673
674 Simoneit, B. R. T., Cox, R. E., and Standley, L. J.: Organic matter of the troposphere - IV. Lipids in
675 harmattan aerosols of Nigeria, Atmos. Environ., 22, 983-1004, https://doi.org/10.1016/0004-
676 6981(88)90276-4, 1967.
677
678 UK-Air, https://uk-air.defra.gov.uk, last accessed 16 December 2018.
679
680 Yee, L. D., Craven, J. S., Loza, C. L., Schilling, K. A., Ng, N. L., Canagaratna, M. R., Ziemann, P.
681 J., Flagan, R. C., and Seinfeld, J. H.: Secondary organic aerosol formation from low-NO_x
682 photooxidation of dodecane: Evolution of multigeneration gas-phase chemistry and aerosol
683 composition, J. Phys. Chem. A., 116, 6211-6230, http://www.doi.org/10.1021/jp211531h, 2012.
684
685 Zhang, H., Worton, D. R., Shen, S., Nah, T., Isaacman-VanWertz, G., Wilson, K. R., and Goldstein,
686 A. H.: Fundamental time scales governing organic aerosol multiphase partitioning and oxidative
687 aging, Environ. Sci. technol., 49, 9768-9777, http://www.doi.org/10.1021/acs.est.5b02115, 2015.
688
689 Zhao, Y., Hu, M., Slanina, S., and Zhang, Y.: The molecular distribution of fine particulate organic
690 matter emitted from Western-style fast food cooking, Atmos. Environ., 41, 8163-8171,
691 http://dx.doi.org/10.1016/j.atmosenv.2007.06.029, 2007a.
692
693 Zhao, Y., Hu, M., Slanina, S., and Zhang, Y.: Chemical compositions of fine particulate organic
694 matter emitted from Chinese cooking, Environ. Sci. Technol., 41, 99-105,
695 http://www.doi.org/10.1021/es0614518, 2007b.
696
697 Ziemann, P. J.: Effects of molecular structure on the chemistry of aerosols formation from the
698 OH-radical-initiated oxidation of alkanes and alkenes, Intl. Rev. Phys. Chem., 30, 161-195,
699 https://doi.org/10.1080/0144235X.2010.550728, 2011.
700
701
702

TABLE LEGENDS

Table 1. The carbon preference index (CPI) and C_{max} for n-alkanals, n-alkan-2-ones, and n-alkan-3-ones in this study and published data.

Table 2. Percentages of particle phase form and the partitioning coefficient Kp.

FIGURE LEGENDS

Figure 1. Map of the sampling sites. RU-Regents University (15 m above ground); WM-University of Westminster (20 m above ground); EL-Eltham; MR-Marylebone Road (south side).

Figure 2. The average total concentration of particle-bound n-alkanals (C_8-C_{20}), n-alkan-2-ones (C_8-C_{26}), and n-alkan-3-ones (C_8-C_{19}), for each sampling period and site. The error bars indicate one standard deviation.

Figure 3. Time series of particle-bound ∑n-alkanals, ∑n-alkan-2-ones and ∑n-alkan-3-ones at RU, WM, EL, and MR sites.

Figure 4. The molecular distribution of particle-bound carbonyl compounds at four sites (RU, WM, EL, and MR).

Table 1. The carbon preference index (CPI) and C_{max} for n-alkanals, n-alkan-2-ones, and n-alkan-3-ones in this study and published data.

Location	Sampling period	n-alkanals		n-alkan-2-ones		n-alkan-3-ones		Reference
Sampling site		CPI	C_{max}	CPI	C_{max}	CPI	C_{max}	
RU, surrounded by Regent's Park, 15 m above ground	23 Jan - 19 Feb	0.52	C_8	1.23	C_{19}	1.30	C_{17}	Present study
WM, 20 m above ground	24 Jan - 20 Feb	0.41	C_8	0.99	C_{20}	1.26	C_{17}	Present study
EL, suburb of London	23 Feb - 21 Mar	0.71	C_8	1.57	C_{20}	1.04	C_{16}	Present study
MR, adjacent to Marylebone road	22 Mar - 18 Apr	1.07	C_8	0.57	C_{16}	1.12	C_{16}	Present study
Athens, Athinas St.	August	1.49	C_{15}, C_{17}	1.09	C_{18}, C_{21}, C_{19}			(Andreou and Rapsomanikis, 2009)
Urban roadside	March			3.26	C_{21}, C_{19}, C_{20}			
Athens, AEDA, Urban, 20 m above ground	March			2.41	C_{19}, C_{18}, C_{20}			(Andreou and Rapsomanikis, 2009)
Heraklion, Greece Urban 15 m above ground	Spring /summer	0.80–1.40	C_{26}, C_{28}	1.30–1.80	C_{23}, C_{29}, C_{31}			(Gogou et al., 1996)
Vancouver, Canada Roadway tunnel				1.33	C_{17}, C_{19}			(Cheng et al., 2006)
Aveiro, Portugal	Summer		C_{22}, C_{23}, C_{26}		C_{26}, C_{28}, C_{30}			
Suburban	Winter							(Oliveira et al., 2007)
K-Puszta, Hungary	Summer		C_{24}, C_{26}, C_{28}		C_{24}, C_{26}, C_{28}			

Table 2. Percentages of particle phase form and the partitioning coefficient Kp (m^3 μg^{-1}).

	RU						WM					
	n-alkanals		n-alkan-2-ones		n-alkan-3-ones		n-alkanals		n-alkan-2-ones		n-alkan-3-ones	
	%	Kp	%	Kp	%	Kp	%	Kp	%	Kp	%	Kp
C_8	82.9	1.16E-04	18.4	5.37E-06	23.9	7.47E-06	80.2	9.09E-05	13.3	3.43E-06	34.1	1.16E-05
C_9	69.2	5.37E-05	14.5	4.03E-06	16.6	4.74E-06	60.5	3.43E-05	15.6	4.16E-06	28.7	9.05E-06
C_{10}	75.3	7.27E-05	13.6	3.77E-06	7.43	1.92E-06	82.1	1.03E-04	14.4	3.77E-06	23.3	6.82E-06
C_{11}	45.5	1.99E-05	21.4	6.49E-06	12.8	3.49E-06	62.4	3.72E-05	20.1	5.65E-06	36.3	1.28E-05
C_{12}	74.8	7.08E-05	25.0	7.96E-06	31.3	1.09E-05	73.7	6.29E-05	28.8	9.07E-06	22.7	6.60E-06
C_{13}	82.9	1.15E-04	61.0	3.74E-05	35.4	1.31E-05	82.2	1.04E-04	48.9	2.14E-05	62.5	3.74E-05
C_{14}	82.8	1.15E-04	49.5	2.34E-05	35.5	1.31E-05	75.8	7.04E-05	31.8	1.05E-05	25.6	7.74E-06
C_{15}	99.5	5.01E-03	84.1	1.26E-04	50.5	2.44E-05	*		85.0	1.27E-04	68.5	4.87E-05
C_{16}	*		91.4	2.53E-04	70.3	5.64E-05	*		89.6	1.93E-04	91.7	2.47E-04
C_{17}	*		91.5	2.55E-04	*		*		85.9	1.36E-04	91.5	2.42E-04
C_{18}	*		94.1	3.80E-04	*		*		84.8	1.26E-04	99.4	4.02E-03
C_{19}	*		99.1	2.69E-03			*		*			
C_{20}	*		*				*		*			
C_{21}			*						*			
C_{22}			*						*			
C_{23}			*						*			
C_{24}			*						*			
C_{25}			*						*			
C_{26}			*						*			

	El						MR					
	n-alkanals		n-alkan-2-ones		n-alkan-3-ones		n-alkanals		n-alkan-2-ones		n-alkan-3-ones	
	%	Kp	%	Kp	%	Kp	%	Kp	%	Kp	%	Kp
C_8	92.7	6.53E-04	24.9	1.72E-05	31.9	2.43E-05	90.0	2.94E-04	28.2	1.28E-05	43.0	2.46E-05
C_9	92.2	6.16E-04	38.0	3.18E-05	44.4	4.15E-05	89.9	2.89E-04	27.0	1.20E-05	39.1	2.09E-05
C_{10}	90.5	4.96E-04	47.6	4.70E-05	47.0	4.59E-05	91.7	3.62E-04	61.1	5.12E-05	20.4	8.33E-06
C_{11}	87.0	3.47E-04	72.3	1.35E-04	81.9	2.34E-04	87.4	2.26E-04	50.2	3.28E-05	33.1	1.61E-05
C_{12}	92.9	6.73E-04	83.4	2.60E-04	66.4	1.02E-04	93.0	4.30E-04	88.5	2.51E-04	28.1	1.28E-05
C_{13}	95.6	1.12E-03	82.2	2.40E-04	65.7	9.92E-05	96.1	8.04E-04	87.7	2.33E-04	46.2	2.79E-05
C_{14}	91.4	5.52E-04	90.3	4.80E-04	59.1	7.48E-05	95.2	6.51E-04	95.9	7.61E-04	72.0	8.38E-05
C_{15}	96.7	1.53E-03	94.5	8.98E-04	84.4	2.80E-04	*		96.9	1.02E-03	83.8	1.69E-04
C_{16}	*		96.7	1.41E-03	89.0	4.18E-04	*		96.4	8.70E-04	88.0	2.38E-04
C_{17}	*		95.1	1.00E-03	81.5	2.28E-04	*		96.0	7.73E-04	88.0	2.39E-04
C_{18}	*		64.6	9.44E-05	85.0	2.93E-04	*		92.5	4.04E-04	*	
C_{19}	*		*				*		*		*	
C_{20}	*		*				*		*			
C_{21}			*						*			
C_{22}			*						*			
C_{23}			*						*			
C_{24}									*			

* For compounds marked with an asterisk, the particulate phase was quantified, but the vapour was below detection limit, and hence K_p is undefined.

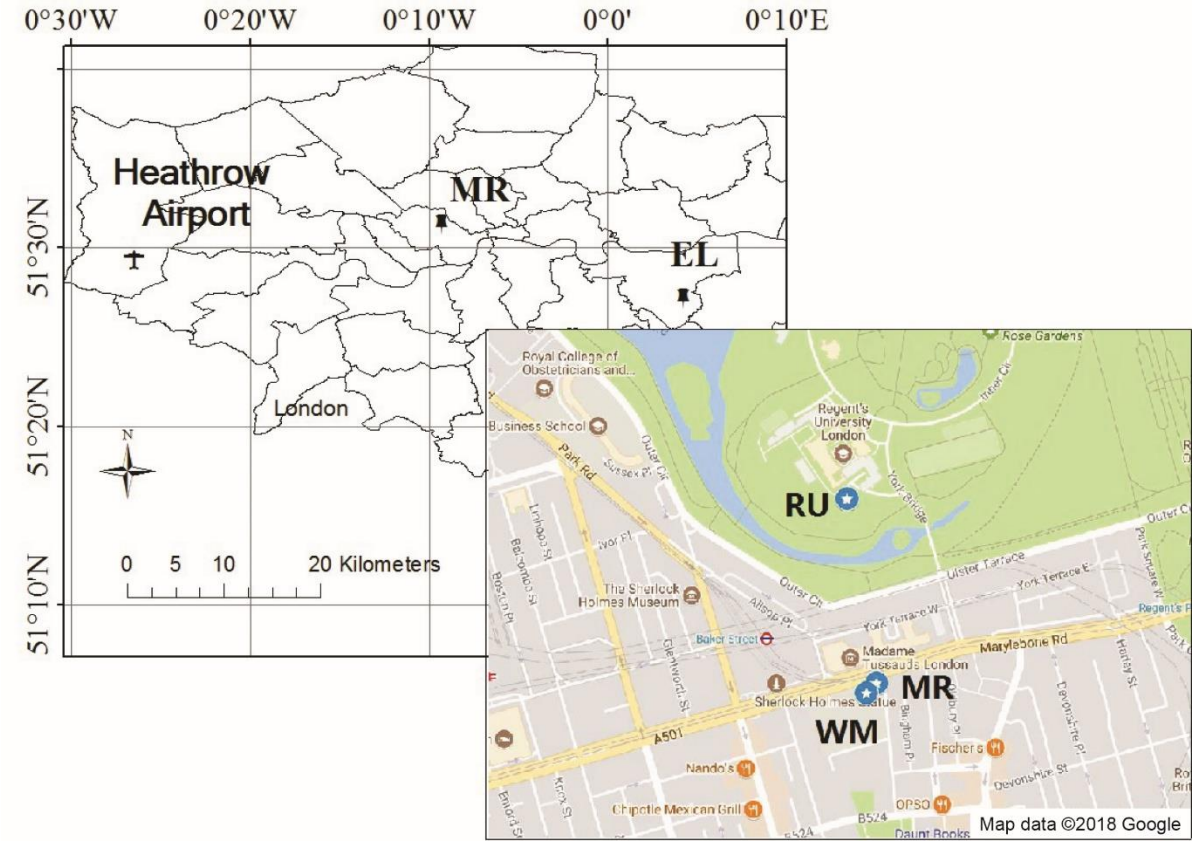

Fig. 1. Map of the sampling sites. RU-Regents University (15 m above ground); WM-University of Westminster (20 m above ground); EL-Eltham; MR-Marylebone Road (south side).

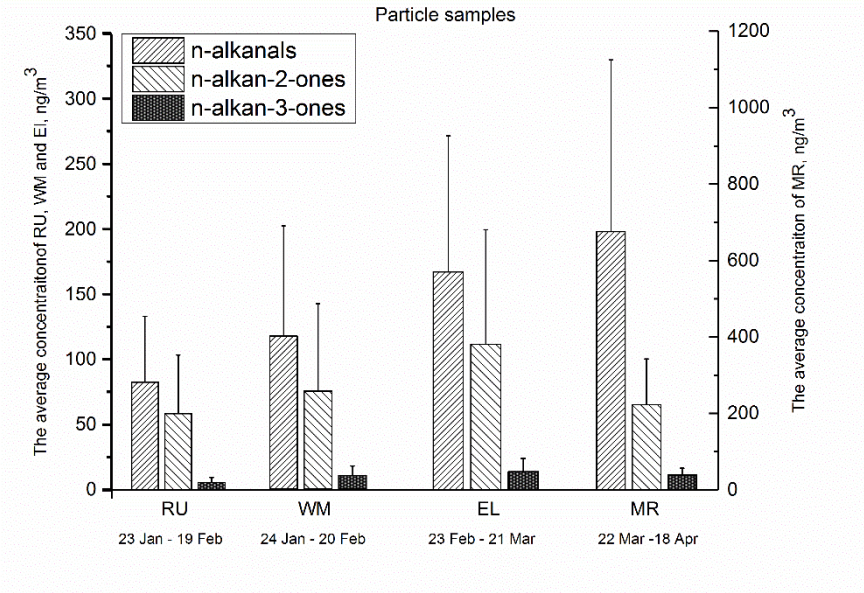

Fig. 2. The average total concentration of particle-bound n-alkanals (C_8-C_{20}), n-alkan-2-ones (C_8-C_{26}), and n-alkan-3-ones (C_8-C_{19}), for each sampling period and site. The error bars indicate one standard deviation.

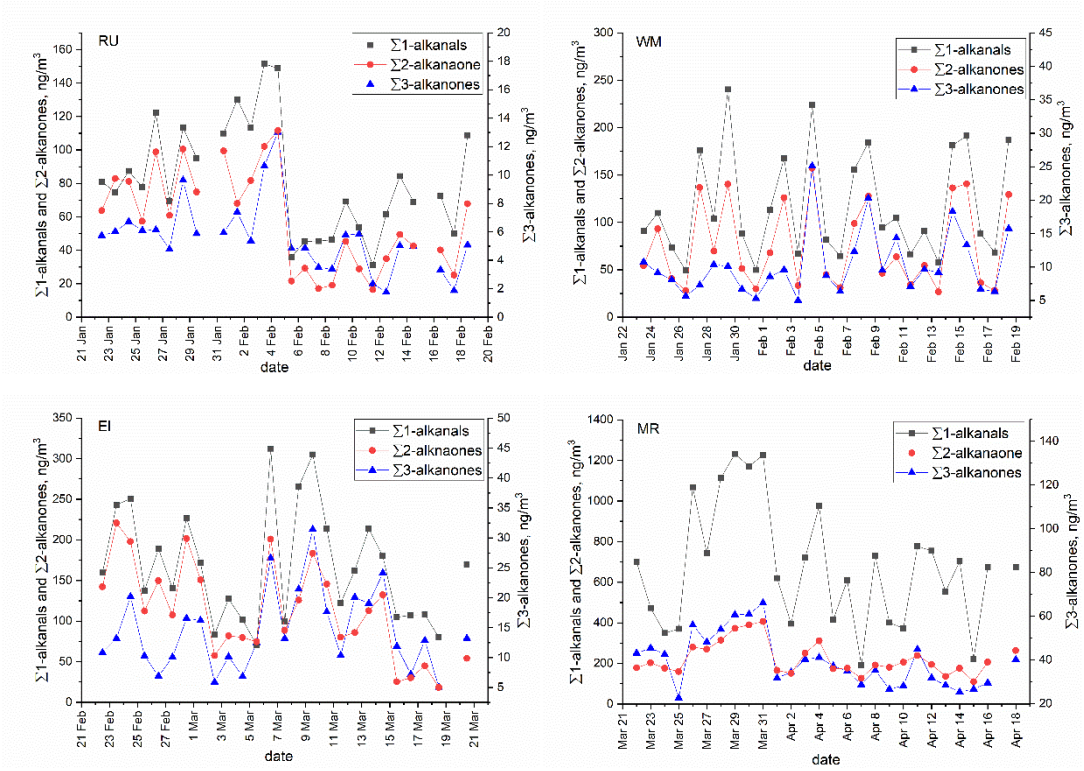

Fig. 3. Time series of particle-bound ∑n-alkanals, ∑n-alkan-2-ones and ∑n-alkan-3-ones at RU, WM, EL, and MR sites.

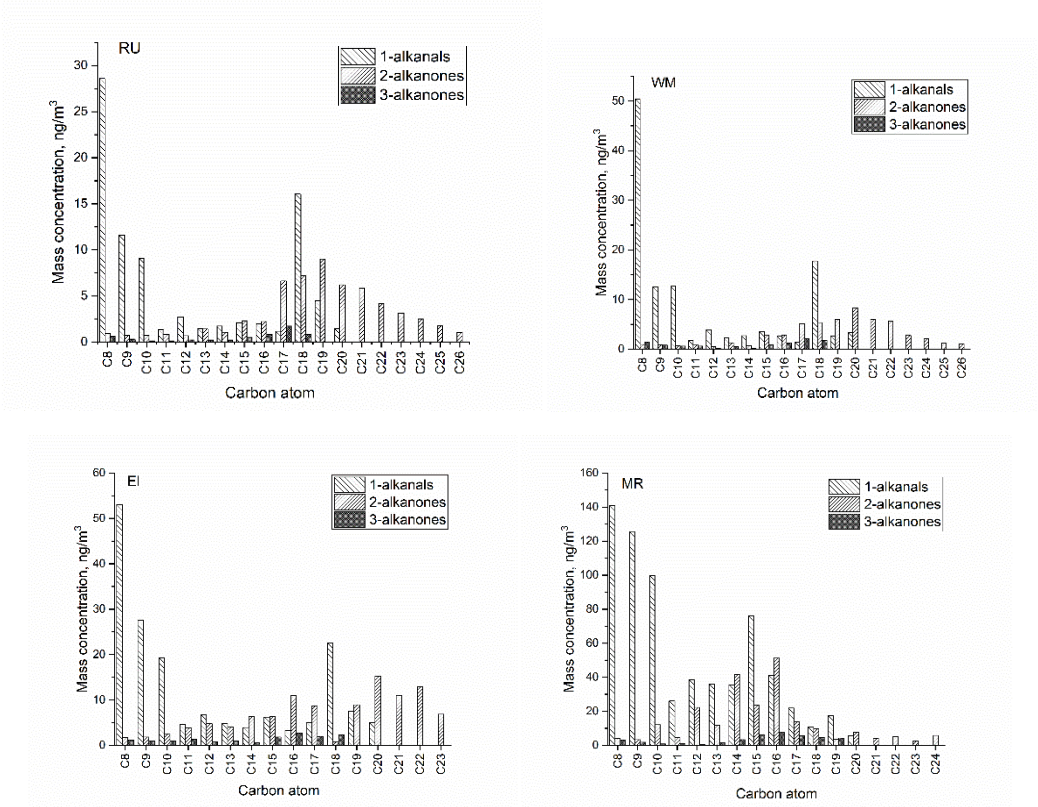

Fig. 4. The molecular distribution of particle-bound carbonyl compounds at four sites (RU, WM, EL, and MR).